Dear Author,

Here are the proofs of your article.

- You can submit your corrections **online**, via **e-mail** or by **fax**.
- For **online** submission please insert your corrections in the online correction form. Always indicate the line number to which the correction refers.
- You can also insert your corrections in the proof PDF and **email** the annotated PDF.
- For fax submission, please ensure that your corrections are clearly legible. Use a fine black pen and write the correction in the margin, not too close to the edge of the page.
- Remember to note the **journal title**, **article number**, and **your name** when sending your response via e-mail or fax.
- **Check** the metadata sheet to make sure that the header information, especially author names and the corresponding affiliations are correctly shown.
- **Check** the questions that may have arisen during copy editing and insert your answers/ corrections.
- **Check** that the text is complete and that all figures, tables and their legends are included. Also check the accuracy of special characters, equations, and electronic supplementary material if applicable. If necessary refer to the *Edited manuscript*.
- The publication of inaccurate data such as dosages and units can have serious consequences. Please take particular care that all such details are correct.
- Please **do not** make changes that involve only matters of style. We have generally introduced forms that follow the journal's style.
  Substantial changes in content, e.g., new results, corrected values, title and authorship are not allowed without the approval of the responsible editor. In such a case, please contact the Editorial Office and return his/her consent together with the proof.
- If we do not receive your corrections **within 48 hours**, we will send you a reminder.
- Your article will be published **Online First** approximately one week after receipt of your corrected proofs. This is the **official first publication** citable with the DOI. **Further changes are, therefore, not possible.**
- The **printed version** will follow in a forthcoming issue.

Please note

After online publication, subscribers (personal/institutional) to this journal will have access to the complete article via the DOI using the URL: http://dx.doi.org/[DOI].
If you would like to know when your article has been published online, take advantage of our free alert service. For registration and further information go to: http://www.link.springer.com.

Due to the electronic nature of the procedure, the manuscript and the original figures will only be returned to you on special request. When you return your corrections, please inform us if you would like to have these documents returned.

Metadata of the article that will be visualized in OnlineFirst

ArticleTitle	Improved Cu_2O/AZO Heterojunction by Inserting a Thin ZnO Interlayer Grown by Pulsed Laser Deposition	
Article Sub-Title		
Article CopyRight	The Minerals, Metals & Materials Society (This will be the copyright line in the final PDF)	
Journal Name	Journal of Electronic Materials	

Corresponding Author	Family Name	**Macaluso**
	Particle	
	Given Name	**R.**
	Suffix	
	Division	Thin Films Laboratory (TFL), Dipartimento di Ingegneria
	Organization	Università degli Studi di Palermo
	Address	Viale delle Scienze (ed. 9), 90128, Palermo, Italy
	Phone	
	Fax	
	Email	roberto.macaluso@unipa.it
	URL	
	ORCID	http://orcid.org/0000-0002-7612-3192
Author	Family Name	**Boughelout**
	Particle	
	Given Name	**A.**
	Suffix	
	Division	
	Organization	Research Centre in Industrial Technologies CRTI
	Address	Algiers, Algeria
	Division	Department of Materials and Compounds, Faculty of Physics
	Organization	USTHB
	Address	BP 32, 16111, Algiers, Algeria
	Phone	
	Fax	
	Email	
	URL	
	ORCID	
Author	Family Name	**Crupi**
	Particle	
	Given Name	**I.**
	Suffix	
	Division	Thin Films Laboratory (TFL), Dipartimento di Ingegneria
	Organization	Università degli Studi di Palermo
	Address	Viale delle Scienze (ed. 9), 90128, Palermo, Italy

	Phone	
	Fax	
	Email	
	URL	
	ORCID	
Author	Family Name	**Megna**
	Particle	
	Given Name	**B.**
	Suffix	
	Division	Laboratorio di Materiali per la Conservazione e il Restauro, Dipartimento di Ingegneria
	Organization	Università degli Studi di Palermo
	Address	Viale delle Scienze (ed. 6), 90128, Palermo, Italy
	Phone	
	Fax	
	Email	
	URL	
	ORCID	
Author	Family Name	**Aida**
	Particle	
	Given Name	**M. S.**
	Suffix	
	Division	Department of Physics, Faculty of Sciences
	Organization	King Abdulaziz University
	Address	Jeddah, Kingdom of Saudi Arabia
	Phone	
	Fax	
	Email	
	URL	
	ORCID	
Author	Family Name	**Kechouane**
	Particle	
	Given Name	**M.**
	Suffix	
	Division	Department of Materials and Compounds, Faculty of Physics
	Organization	USTHB
	Address	BP 32, 16111, Algiers, Algeria
	Phone	
	Fax	
	Email	
	URL	
	ORCID	

Schedule	Received	26 October 2018
	Revised	

Accepted 4 April 2019

Abstract

Cu_2O/ZnO:Al (AZO) and Cu_2O/ZnO/AZO heterojunctions have been deposited on glass substrates by a unique three-step pulsed laser deposition process. The structural, optical, and electrical properties of the oxide films were investigated before their implementation in the final device. X-ray diffraction analysis indicated that the materials were highly crystallized along the *c*-axis. All films were highly transparent in the visible region with enhanced electrical properties. Atomic force and scanning electron microscopies showed that the insertion of a ZnO layer between the Cu_2O and AZO films in the heterojunction enhanced the average grain size and surface roughness. The heterojunctions exhibited remarkable diode behavior and good rectifying character with low leakage current under reverse bias. The presence of the ZnO interlayer film significantly reduced the parasitic and leakage currents across the barrier, improved the quality of the heterostructure, made the energy band between AZO and Cu_2O layers smoother, and eliminated the possibility of interface recombination, leading to much longer electron lifetime.

Keywords (separated by '-') Heterojunctions - thin films - ZnO - Cu_2O - AZO - pulsed laser deposition - solar cells

Footnote Information

Journal of ELECTRONIC MATERIALS
https://doi.org/10.1007/s11664-019-07195-6

Improved Cu_2O/AZO Heterojunction by Inserting a Thin ZnO Interlayer Grown by Pulsed Laser Deposition

A. BOUGHELOUT,[1,2] R. MACALUSO,[3,6] I. CRUPI,[3] B. MEGNA,[4] M.S. AIDA,[5] and M. KECHOUANE[2]

1.—Research Centre in Industrial Technologies CRTI, Algiers, Algeria. 2.—Department of Materials and Compounds, Faculty of Physics, USTHB, BP 32, 16111 Algiers, Algeria. 3.—Thin Films Laboratory (TFL), Dipartimento di Ingegneria, Università degli Studi di Palermo, Viale delle Scienze (ed. 9), 90128 Palermo, Italy. 4.—Laboratorio di Materiali per la Conservazione e il Restauro, Dipartimento di Ingegneria, Università degli Studi di Palermo, Viale delle Scienze (ed. 6), 90128 Palermo, Italy. 5.—Department of Physics, Faculty of Sciences, King Abdulaziz University, Jeddah, Kingdom of Saudi Arabia. 6.—e-mail: roberto.macaluso@unipa.it

Cu_2O/ZnO:Al (AZO) and Cu_2O/ZnO/AZO heterojunctions have been deposited on glass substrates by a unique three-step pulsed laser deposition process. The structural, optical, and electrical properties of the oxide films were investigated before their implementation in the final device. X-ray diffraction analysis indicated that the materials were highly crystallized along the *c*-axis. All films were highly transparent in the visible region with enhanced electrical properties. Atomic force and scanning electron microscopies showed that the insertion of a ZnO layer between the Cu_2O and AZO films in the heterojunction enhanced the average grain size and surface roughness. The heterojunctions exhibited remarkable diode behavior and good rectifying character with low leakage current under reverse bias. The presence of the ZnO interlayer film significantly reduced the parasitic and leakage currents across the barrier, improved the quality of the heterostructure, made the energy band between AZO and Cu_2O layers smoother, and eliminated the possibility of interface recombination, leading to much longer electron lifetime.

Key words: Heterojunctions, thin films, ZnO, Cu_2O, AZO, pulsed laser deposition, solar cells

INTRODUCTION

Over recent decades, transparent conductive oxides (TCOs) have attracted considerable scientific attention and technological interest as an indispensable element in many optoelectronic applications. Due to the coexistence of high transparency and excellent conductivity, TCO materials pervade modern technologies, being a critical component of displays, touchscreens, lighting devices, and solar cells.[1,2]

Zinc oxide (ZnO) and its aluminum-doped variant (AZO) are among the most widely utilized TCO thin films thanks to their abundance in Nature, nontoxicity, and low cost. It is well known that, due to oxygen vacancies and zinc interstitials, ZnO behaves like an *n*-type semiconductor with a wide bandgap (about 3.3 eV) and that Al doping is normally performed to enhance its electrical conductivity, making AZO ideal for contacts in solar cells.[3] On the other hand, due to Cu vacancies in the lattice, cuprous oxide (Cu_2O) is intrinsically *p*-type, showing good optical properties and a bandgap of about 2.1 eV,[4] which is good for use as the absorber layer in photovoltaic devices. However, the intrinsic *p*-type nature of Cu_2O makes formation of a homojunction impossible, thus hindering achievement of the maximum efficiency.[5]

Cu_2O/ZnO or Cu_2O/AZO heterojunctions, with theoretically conversion efficiency of around 20%,[6]

(Received October 26, 2018; accepted April 4, 2019)

are some of the most attractive candidates for use in next-generation thin-film-based solar cells,[7] because of the comparatively favorable alignment of the conduction-band edges[8] and use of Earth-abundant elements.[9–17] Experimental efficiencies of 1.46%, 1.43%, and 0.3% have been reported when using Cu_2O and ZnO layers obtained by atmospheric atomic-layer deposition (AALD),[9] electrodeposition,[15] and electrodeposition and spin coating,[16] respectively. Over recent years, to improve the conversion efficiency of solar cells, the Cu_2O/AZO/ZnO heterostructure has been proposed[18–23] and efficiencies up to 4.08% reported.[18] Although Cu_2O/AZO or Cu_2O/ZnO heterojunctions have already been widely studied,[9–17] their behavior on insertion of a ZnO thin film within the Cu_2O/AZO stack has been reported in only a few works.[18–23] Furthermore, in those studies, distinct techniques were employed to grow the different layers constituting the heterostructure. In particular, in Refs. [18–20], AZO and ZnO films were deposited by PLD, whilst Cu_2O films were obtained by thermal oxidation of a Cu sheet. In Ref. [21] instead, ZnO and AZO thin films were deposited by ALD while the Cu_2O layer was obtained by electrodeposition. In Ref. [22], all the Cu_2O/AZO/ZnO heterojunction was fabricated using a three-step electrodeposition process, and finally in Ref. [23], magnetron sputtering was used for the deposition of AZO and ZnO thin films, whilst the Cu_2O layer was grown by metalorganic chemical vapor deposition (MOCVD).

In the work presented herein, we obtained the full Cu_2O/AZO/ZnO stack structure after a unique three-step pulsed laser deposition (PLD) process,[24–29] making the fabrication process simpler and decreasing the damage compared with other literature reports[18–23] and further improving the quality of the heterojunction in terms of the interface, surface roughness, passivation, and leakage currents. Study of the morphological, structural, optical, and electrical properties of the deposited Cu_2O/AZO and Cu_2O/ZnO/AZO heterojunctions revealed that the *p*-Cu_2O/*n*-ZnO/*n*-AZO heterojunctions exhibited well-defined rectifying behavior and could thus be useful for future high-performance heterostructure photovoltaic devices.

EXPERIMENTAL PROCEDURES

Sample Preparation

Corning glass substrates with dimensions of 1 cm × 2 cm were ultrasonically cleaned with acetone and ethanol for 10 min. Afterwards, Ti/Au bottom contacts were deposited by thermal evaporation. Cu_2O/AZO and Cu_2O/ZnO/AZO heterojunctions were then deposited by PLD using a Q-switched tripled Nd:YAG laser (Quantel mod.-YG78C20, λ = 355 nm).[24–29] The laser beam, with energy density of 4 J/cm^2 and repetition rate of 20 Hz, was focused at an angle of incidence of 25° onto the target, which was in turn placed on an *x*–*y* translation system to enable uniform ablation of its surface. The ZnO target (99.999% pure) and AZO target (99.9% pure) were 2-inch-diameter, 0.25-inch-thick, sintered zinc oxide ceramic disks supplied by CERAC Inc. (USA) and PI-KEM Ltd., respectively, while the Cu_2O target was obtained by cold pressing Cu_2O powder (purity 99.99%, Sigma Aldrich). All films were deposited with oxygen pressure of 10^{-2} mbar. Cu_2O films were deposited at room temperature, whilst ZnO and AZO films were deposited at 150°C to avoid degradation of the electrical properties of the underlying Cu_2O film.[30] Glass substrate was employed as a reference sample during each film deposition and for further analysis.

Characterization Techniques

X-ray diffraction (XRD) measurements were performed using a PANalytical Empyrean powder x-ray diffractometer with copper anode (Cu K_α radiation, λ = 0.15405 nm, with Ni filter) equipped with a PIXCel^{1D} detector, at 40 kV and 40 mA. XRD patterns were recorded over the 2θ angle range from 25° to 80° at step size of 0.026° and speed of 4°/min. Raman spectra of all films were recorded using a Renishaw InVia Raman microscope, equipped with a 532-nm diode pulsed solid-state laser, focused on the sample by means of a Leica MS-DS microscope through a 50× magnification long-working-distance lens, capable of 4 μm lateral resolution, edge filter cutting Rayleigh reflection at 125 cm^{-1}, and 2400-line/mm grating leading to spectral resolution of 0.5 cm^{-1}. The surface morphology of the films was analyzed by field-emission scanning electron microscopy (SEM) using a Zeiss Supra 25 microscope and atomic force microscopy (AFM) using a Bruker ICON equipped with PeakForce mode at scan rate of 0.6 Hz and tapping mode at scan rate of 0.8 Hz.

Optical transmission measurements were performed using a Cary 500 ultraviolet–visible–near infrared (UV–Vis–NIR) spectrophotometer in the range from 250 nm to 2500 nm with resolution of 0.3 nm in the UV–Vis wavelength region and 1 nm in the NIR. The film thickness was determined using a SEMILAB GES-5E spectroscopic ellipsometer and is summarized in Table I together with the resistivity, carrier concentration, and mobility values identified by the van der Pauw method, employing a commercial Hall measurement system (ECOPIA HMS-3000).

I–*V* characterization of the heterojunctions was performed at room temperature using a custom-developed electronic circuit which allowed the voltage to be swept in the range from −10 V to 10 V.[28]

RESULTS AND DISCUSSION

Oxide Films

Figure 1 shows the XRD patterns of the films deposited on glass substrates, recorded in θ–2θ configuration. Both the AZO and ZnO samples

Journal : 11664_JEM Dispatch : 9-4-2019 Pages : 8
Article No.: 7195 ☐ LE ☑ CP ☐ TYPESET ☑ DISK

Table I. Film thickness (extracted by ellipsometry), electrical properties (by Hall measurements), and optical bandgap energy (by Tauc plot) of AZO, ZnO, and Cu_2O films grown on glass substrates

Film	Thickness (nm)	Carrier Concentration (cm^{-3})	Resistivity (Ω cm)	Mobility ($cm^2 V^{-1} s^{-1}$)	Bandgap (eV)
Cu_2O	210	$+3.6 \times 10^{14}$	2.4×10^{2}	71.38	2.20
AZO	220	-6.7×10^{20}	2.6×10^{-4}	35.23	3.43
ZnO	150	-2.2×10^{19}	7.3×10^{-3}	38.21	3.20

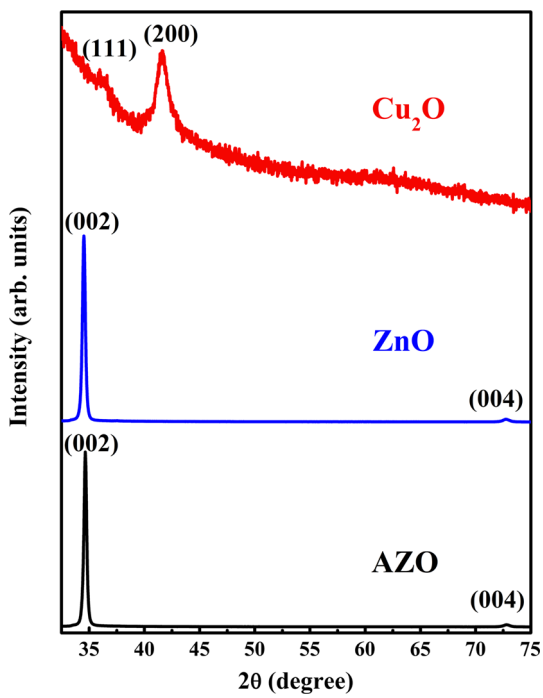

Fig. 1. XRD patterns of Cu_2O, ZnO, and AZO thin films grown on glass substrates.

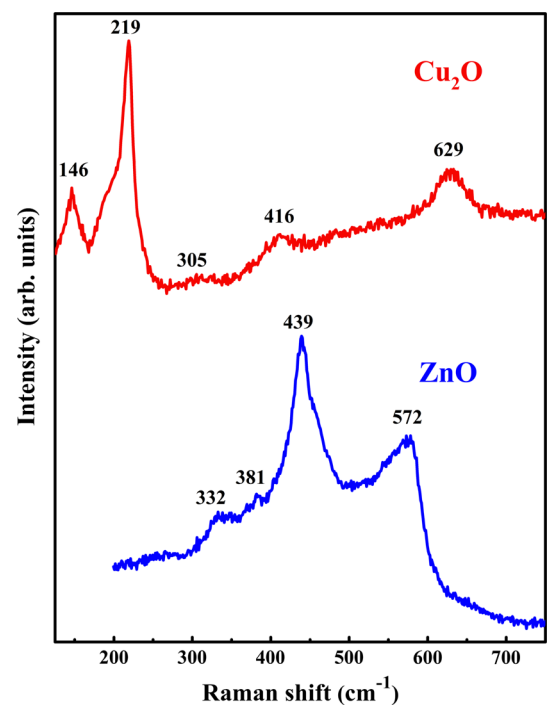

Fig. 2. Raman spectra of Cu_2O and ZnO thin films grown on glass substrates.

presented a ZnO phase, highly textured along the *c*-axis perpendicular to the substrate surface, with a significant (002) peak located at about 34.60° according to Joint Committee on Powder Diffraction Standards (JCPDS) card no. 036-1451[31] with high intensity for all deposited samples, confirming the hexagonal wurtzite structure of the films. This result can be explained by the fact that the (002) plane requires a lower energy of formation.[32] The Cu_2O films were also highly crystallized along the *c*-axis but with a significant (200) peak located at about 41.61° and a small peak located at about 36.61° corresponding to the (111) crystal planes of Cu_2O cubic phase (JCPDS card no. 05–0667).[33] The average crystallite size of the films was estimated using the Scherrer formula,[34]

$$D = 0.9\frac{\lambda}{W\cos(\theta)}, \quad (1)$$

where D, λ, θ, and W are the mean grain size, x-ray wavelength (0.154 nm), Bragg diffraction angle, and full-width at half-maximum (FWHM) of the diffraction peak, respectively. The average crystallite size of single-crystalline domains was obtained as 33 nm, 31 nm, and 9.5 nm for AZO, ZnO, and Cu_2O, respectively.

These XRD results are in good agreement with Raman spectroscopy. Phonon modes with characteristic frequencies of crystalline Cu_2O and ZnO are evident in Fig. 2. Five peaks are observed in the Raman spectrum of the Cu_2O film. The highest peak, located at 219 cm^{-1}, is attributed to the second-order Raman-allowed mode 2_{Eu} of Cu_2O phase, while that with low intensity at around 305 cm^{-1} is attributed to the second-order overtone mode A_{2u} while the peak located at 416 cm^{-1} corresponds to the four-phonon mode $3E_u + T_{2u}$.[35,36] The peaks located at 146.33 cm^{-1} and 629 cm^{-1} correspond instead to two infrared-allowed modes.[37] The Raman spectrum of the ZnO film shows four peaks. The first, located at 573 cm^{-1}, corresponds to the A1 longitudinal optical (LO) mode, which can be attributed to lattice distortion.[38,39] The highest

Journal : 11664_JEM Dispatch : 9-4-2019 Pages : 8
Article No.: 7195 ☐ LE ☑ CP ☐ TYPESET ☑ DISK

peak, centered at 439 cm^{-1}, may be assigned to the ZnO E_2(high) mode, which indicates the high crystalline quality of the film, being a characteristic band of hexagonal wurtzite phase.[39–41] The peak at 382 cm^{-1} corresponds to the A1 (TO) mode of wurtzite ZnO crystal.[38,42–44] The final peak, at 332 cm^{-1}, can be attributed to the E_2(high) – E_2(low) mode due to multiphonon process, indicating that the films were single crystals.[39] These data provide evidence that PLD allows deposition of good-quality ZnO and Cu_2O thin films.

Figure 3a shows the transmission spectra of AZO, ZnO, and Cu_2O films deposited on glass in the wavelength range from 250 nm to 2500 nm. The undoped zinc oxide film was highly transparent with optical transmittance as high as 80% to 90% in the Vis–NIR and an absorption edge at about 375 nm. The most significant difference from the AZO curve can be observed in the NIR spectral region, where a pronounced drop, caused by free-carrier absorption, is visible for the AZO film. Also, the Cu_2O film showed high transmittance of up to 85% in the range from 650 nm to 2500 nm. A few interference fringes can be observed in the transmittance spectra, indicating weak surface roughness.[45] The optical bandgap energy, E_g, of the materials was evaluated using the Tauc relation,[22,46]

$$(\alpha h\upsilon)^2 = B(h\upsilon - E_g), \quad (2)$$

where α is the absorption coefficient, $h\upsilon$ is the photon energy, and B is the Tauc coefficient, related to the light absorption efficiency. From the intercept of the straight-line portion of the curves at $\alpha = 0$ in the Tauc plot [47] in Fig. 3b, energy gaps of 3.20 eV, 3.43 eV, and 2.20 eV were estimated for ZnO, AZO, and Cu_2O (Table I), respectively, in good agreement with literature. Also, the electrical properties of the films (Table I) are very close to literature values.[48] As expected, n-type zinc oxide films have carrier concentration much higher and resistivity much lower than p-type Cu_2O samples.[49]

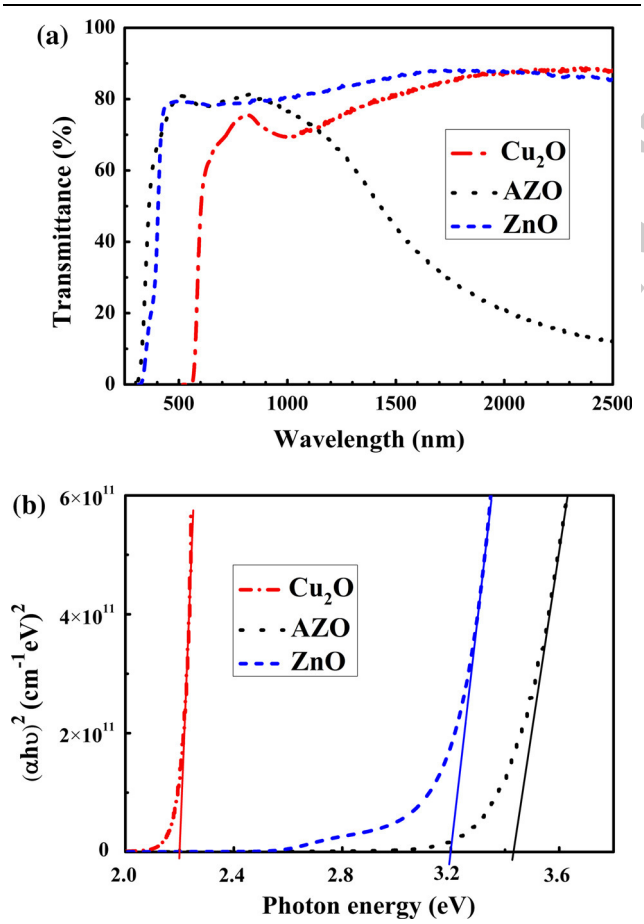

Fig. 3. (a) Optical transmittance spectra of ZnO, AZO, and Cu_2O thin films grown on glass substrates and (b) corresponding Tauc plots for determination of the optical bandgap.

Heterojunctions

A typical cross-sectional view of the Cu_2O/AZO heterojunction is shown in Fig. 4a. The bilayer Cu_2O/AZO structure is clear, and both films are uniform with thickness in agreement with the ellipsometric measurements. However, while the presence of the ZnO interlayer, due to its similar lattice structure and mismatch (Fig. 1) with AZO, cannot be evidenced from the images in cross-section, it changes the surface morphology of the AZO on top. The plan-view images reveal that the top surface of the Cu_2O/ZnO/AZO structure (Fig. 4b) was rougher than that of the Cu_2O/AZO structure (Fig. 4c). This change in the morphology is due to the formation of nucleation sites and the change in the nucleation type from homogeneous to heterogeneous when the AZO film is deposited on ZnO and Cu_2O, respectively. The presence of surface texture will play a significant role in the performance of the solar cell, since it will reduce the reflection loss at its front surface, enhance the light absorption, and increase the photocurrent.

Since the morphology (porosity and roughness) of the heterojunction surface is very important for photovoltaic applications, AFM characterization in tapping mode was carried out and the surface roughness and grain size of the films calculated using the NanoScope analysis program. Figure 5 shows three-dimensional (3D) and two-dimensional (2D) AFM images of Cu_2O/ZnO/AZO and Cu_2O/AZO heterojunctions, confirming that insertion of the ZnO layer between the Cu_2O and AZO films led to an increase in both the average grain size (from 62 nm to 96 nm, Fig. 5a and b) and the surface roughness (defined by the root-mean-square roughness, from 16.5 nm to 19.5 nm). An increase of the porosity is also evident in Fig. 5c and d. It is worth mentioning that larger grains imply fewer grain boundaries and thus enhanced device performance. This is due to the fact that grain boundaries, acting

Journal : 11664_JEM Dispatch : 9-4-2019 Pages : 8
Article No.: 7195 ☐ LE ☑ CP ☐ TYPESET ☑ DISK

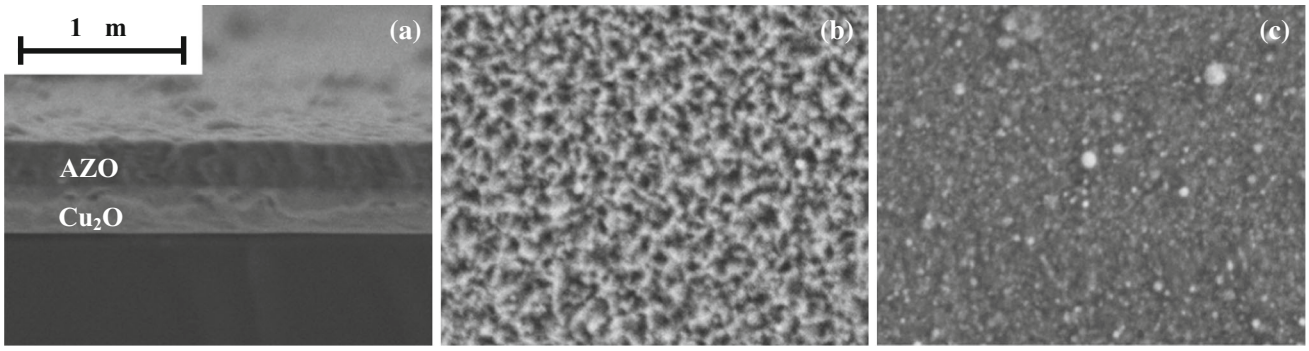

Fig. 4. Typical SEM images of: (a) Cu_2O/AZO heterojunction in cross-section, (b) Cu_2O/ZnO/AZO and (c) Cu_2O/AZO in plan view. The scale marker in (a) applies to all three images.

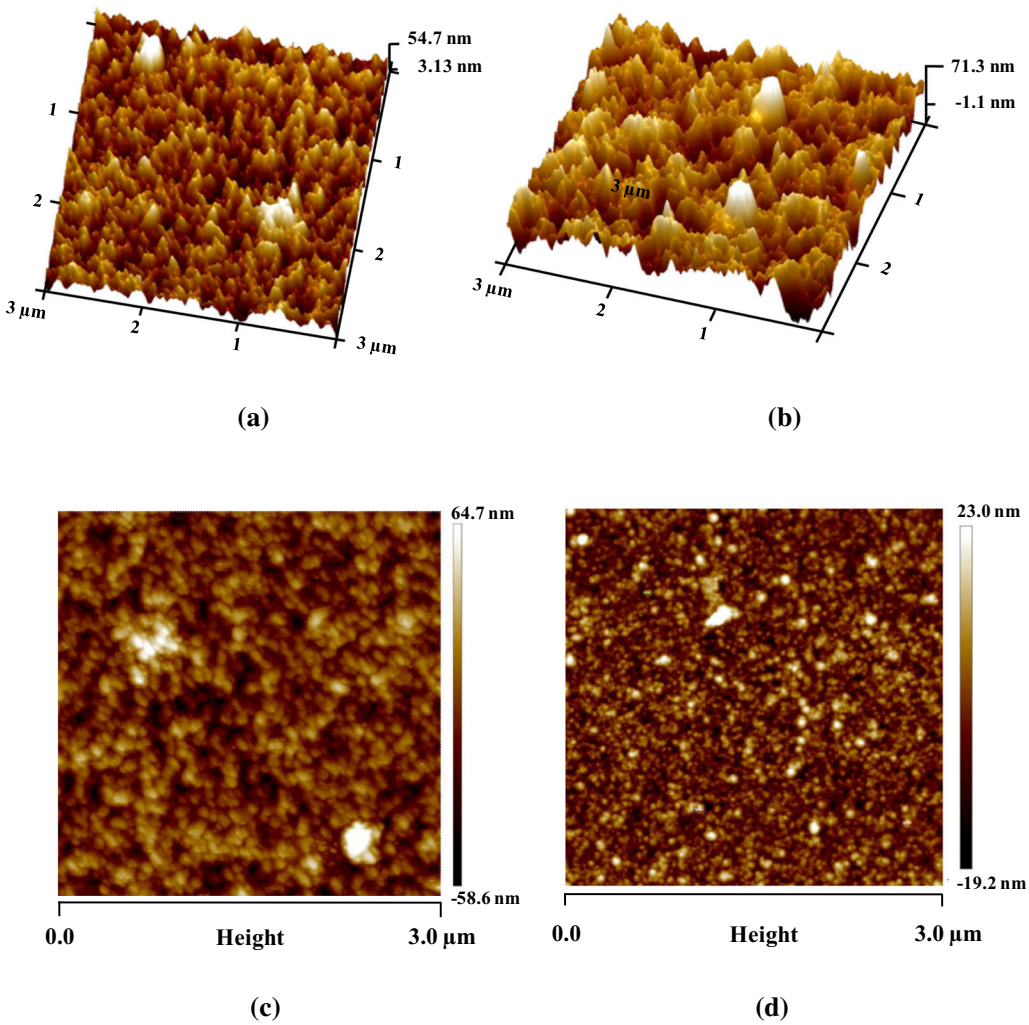

Fig. 5. Tapping-mode 3D and 2D AFM images (3 μm $\times$ 3 μm) of Cu_2O/AZO (a, c) and Cu_2O/ZnO/AZO (b, d) heterojunctions.

as recombination sites for photocarriers, lead to efficiency losses.

To investigate the electrical properties of the heterojunctions, 1-mm-diameter aluminum (Al) contact layers were deposited on top of the AZO layers of the Au/Cu_2O/AZO and Au/Cu_2O/ZnO/AZO sandwich structures. The AZO/Al and Au/Cu_2O contacts were perfectly ohmic. Figure 6 shows the current–voltage (I–V) curves for the Au/Cu_2O/AZO/Al and Au/Cu_2O/ZnO/AZO/Al structures. A defined diode-like rectifying nature with lower reverse saturation current (I_0), due to the reduced interface recombination, is clearly observed in the sample with the ZnO buffer layer, implying that this device would

Journal : 11664_JEM Dispatch : 9-4-2019 Pages : 8
Article No.: 7195 ☐ LE ☑ CP ☐ TYPESET ☑ DISK

exhibit improved photovoltaic properties under illumination. Indeed, a reduction of I_0 is known to enhance the open-circuit voltage (V_{OC}) and fill factor (FF) of a solar cell.[50] I_0 is reduced in the presence of the buffer layer thanks to the passivation of interface defects where recombination occurs.

Based on the measured bandgap values and considering the electron affinity (χ) of Cu_2O, ZnO, and AZO (3.2 eV, 4.2 eV, and 4.6 eV, respectively),[22,51,52] an energy band diagram for the Cu_2O/AZO and Cu_2O/ZnO/AZO heterojunctions can be constructed (Fig. 7). The calculated conduction (ΔE_c) and valence (ΔE_v) band offset of the Cu_2O/AZO heterojunction are 1.4 eV and 2.63 eV, respectively, whilst for the Cu_2O/ZnO heterojunction they are 1.0 eV and 2 eV, respectively. The effective energy gap (E_{eff}) of the Cu_2O/AZO structure, defined as the energy difference between the E_c of AZO and the E_v of Cu_2O, is about 0.8 eV. This very low value may cause interface recombination between holes coming from the Cu_2O layer and electrons coming from the AZO layer. However, the E_{eff} of the Cu_2O/ZnO/AZO structure, viz. the energy difference between the E_c of the ZnO and the E_v of Cu_2O, is about 1.2 eV. Such a larger value could be useful to eliminate the possibility of interface recombination between holes from the Cu_2O film and electrons from the ZnO film.[21,53,54] The presence of the ZnO interfacial layer leads to a cascaded energy level in the sandwiched structure, having $E_c(AZO) < E_c(ZnO) < E_c(Cu_2O)$ and $E_v(AZO) < E_v(ZnO) < E_v(Cu_2O)$. This results in a driving force through the different layers of the device, being advantageous for carrier transport towards the electrodes.[55]

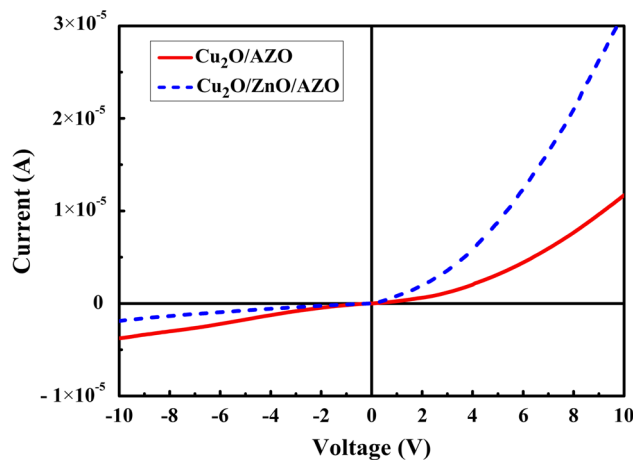

Fig. 6. *I–V* characteristics of Au/Cu_2O/AZO/Al and Au/Cu_2O/ZnO/AZO/Al heterojunctions.

CONCLUSIONS

We used a unique three-step PLD process to deposit thin-film Cu_2O/AZO and Cu_2O/ZnO/AZO heterojunctions on Corning glass, at temperature of 150°C for AZO and ZnO films and room temperature for Cu_2O films. The Cu_2O layers were *p*-type semiconductors with concentration of 3.6×10^{14} cm^{-3} and resistivity of 2.4×10^2 Ω cm. The AZO and ZnO layers were *n*-type semiconductors with carrier concentration of 6.7×10^{20} cm^{-3} and 2.2×10^{19} cm^{-3}, and resistivity of 2.6×10^{-4} Ω cm and 7.3×10^{-3} Ω cm, respectively. All the layers were transparent in the visible wavelength range with transmissivity above 80%.

I–V measurements revealed remarkable diode behavior and good rectifying character with low leakage current under reverse bias. Insertion of a ZnO film within the Cu_2O/AZO structure enhanced

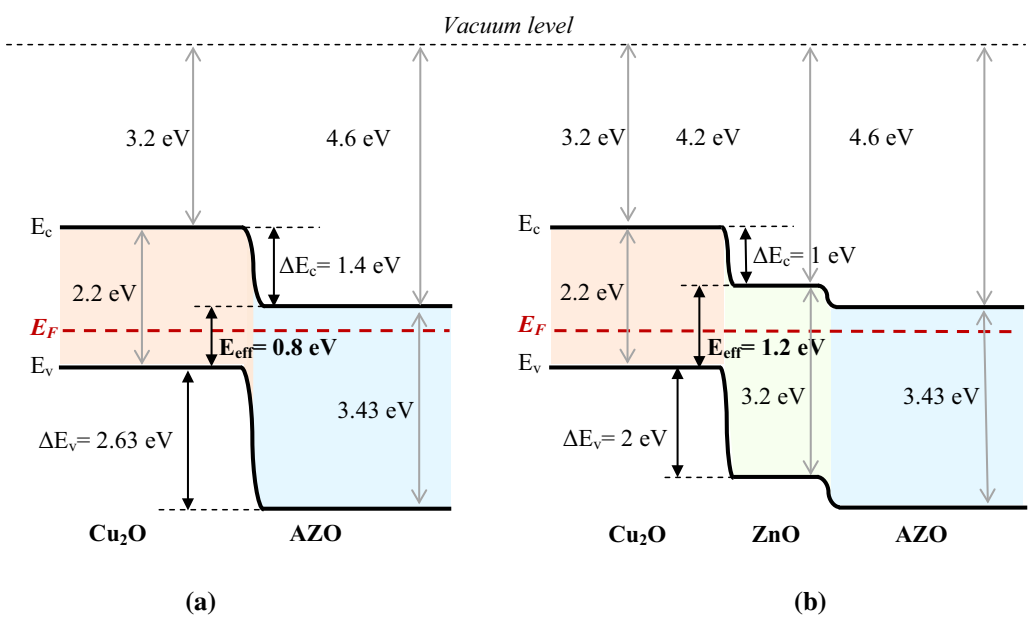

Fig. 7. Schematic band diagram of Cu_2O/AZO and Cu_2O/ZnO/AZO heterojunctions under equilibrium condition.

Journal : 11664_JEM Dispatch : 9-4-2019 Pages : 8
Article No.: 7195 ☐ LE ☑ CP ☐ TYPESET ☑ DISK

the average grain size and surface roughness, significantly limited the parasitic and leakage currents across the barrier, and improved the quality of the heterostructure. The ZnO interlayer increased the effective energy gap from 0.8 eV to 1.2 eV with a reduction in interfacial recombination between holes from the Cu_2O film and electrons from the ZnO film. Finally, the presence of the ZnO film led to a cascaded energy level in the sandwiched structure, enabling an increase of the electron lifetime. Passivation of interface defects between the Cu_2O and AZO films by insertion of a ZnO layer could thus improve the performance of solar cells that make use of this kind of heterojunction.

ACKNOWLEDGMENTS

The authors are grateful to Prof. M. Santamaria (Dipartimento di Ingegneria, Università degli Studi di Palermo) for the use of the XRD system and to CNR-IMM Catania (University) for the use of the SEM.

REFERENCES

1. D.S. Ginley, H. Hosono, and D.C. Paine, *Handbook of Transparent Conductors* (Berlin: Springer, 2010).
2. G. Torrisi, I. Crupi, S. Mirabella, and A. Terrasi, *Sol. Energy Mater. Sol. Cells* 165, 88 (2017).
3. M. Mosca, R. Macaluso, F. Caruso, V. Lo Muzzo, and C. Cali, *Advances in Semiconductor Research: Physics of Nanosystems, Spintronics and Technological Applications*, ed. D. Persano Adorno and S. Pokutnyi (New York: Nova Science, 2015), pp. 245–282.
4. M. Nolan and S.D. Elliott, *Phys. Chem. Chem. Phys.* 8, 5350 (2006).
5. D.O. Scanlon and G.W. Watson, *J. Phys. Chem. Lett.* 1, 2582 (2010).
6. B. Meyer, A. Polity, D. Reppin, M. Becker, P. Hering, P. Klar, T. Sander, C. Reindl, J. Benz, and M. Eickhoff, *Phys. Status Solidi B* 249, 1487 (2012).
7. T.K.S. Wong, S. Zhuk, S. Masudy-Panah, and G.K. Dalapati, *Materials* 9, 271 (2016).
8. S. Jeong, A. Mittiga, E. Salza, A. Masci, and S. Passerini, *Electrochim. Acta* 53, 2226 (2008).
9. Y. Ievskaya, R.L.Z. Hoye, A. Sadhanala, K.P. Musselman, and J.L. MacManus-Driscoll, *Sol. Energy Mater. Sol. Cells* 135, 43 (2015).
10. H. Lahmar, F. Setifi, A. Azizi, G. Schmerber, and A. Dinia, *J. Alloys Compd.* 718, 36 (2017).
11. M. Abdelfatah, J. Ledig, A. El-Shaer, A. Wagner, V. Marin-Borras, A. Sharafeev, P. Lemmens, M.M. Mosaad, A. Waag, and A. Bakin, *Sol. Energy Mater. Sol. Cells* 145, 454 (2016).
12. M. Willander, O. Nur, Q. Zhao, L. Yang, M. Lorenz, B. Cao, J.Z. Pérez, C. Czekalla, G. Zimmermann, and M. Grundmann, *Nanotechnology* 20, 332001 (2009).
13. K. Akimoto, S. Ishizuka, M. Yanagita, Y. Nawa, G.K. Paul, and T. Sakurai, *Sol. Energy* 80, 715 (2006).
14. J.B. Cui and U.J. Gibson, *Phys. Chem. C* 114, 6408 (2010).
15. K. Fujimoto, T. Oku, and T. Akiyama, *Appl. Phys. Express* 6, 086503 (2013).
16. T. Oku, T. Yamada, K. Fujimoto, and T. Akiyama, *Coatings* 4, 203 (2014).
17. M. Izaki, T. Shinagawa, K.-T. Mizuno, Y. Ida, M. Inaba, and A. Tasaka, *J. Phys. D Appl. Phys.* 40, 3326 (2007).
18. Y. Nishi, T. Miyata, and T. Minami, *J. Vac. Sci. Technol. A* 30, 04D103 (2012).
19. T. Minami, Y. Nishi, T. Miyata, and J. Nomoto, *Appl. Phys. Express* 4, 062301 (2011).
20. Y. Nishi, T. Miyata, and T. Minami, *Thin Solid Films* 528, 72 (2013).
21. Y.S. Lee, J. Heo, S.C. Siah, J.P. Mailoa, R.E. Brandt, S.B. Kim, R.G. Gordon, and T. Buonassisi, *Energy Environ. Sci.* 6, 2112 (2013).
22. H. Lahmar, A. Azizi, G. Schmerber, and A. Dinia, *RSC Adv.* 73, 68663 (2016).
23. S.H. Jeong, S.H. Song, K. Nagaich, S.A. Campbell, and E.S. Aydil, *Thin Solid Films* 519, 6613 (2011).
24. M. Barbouche, R.B. Zaghouani, N.E. Benammar, V. Aglieri, M. Mosca, R. Macaluso, K. Khirouni, and H. Ezzaouia, *Superlattices Microstruct.* 101, 512 (2017).
25. A. Sacco, M.S. Di Bella, M. Gerosa, A. Chiodoni, S. Bianco, M. Mosca, R. Macaluso, C. Calì, and C.F. Pirri, *Thin Solid Films* 574, 38 (2015).
26. M. Mosca, R. Macaluso, C. Calì, R. Butté, S. Nicolay, E. Feltin, D. Martin, and N. Grandjean, *Thin Solid Films* 539, 55 (2013).
27. R. Macaluso, M. Mosca, C. Calì, F. Di Franco, M. Santamaria, F. Di Quarto, and J.-L. Reverchon, *J. Appl. Phys.* 113, 164508 (2013).
28. R. Macaluso, M. Mosca, V. Costanza, A. D'angelo, G. Lullo, F. Caruso, C. Calì, F. Di Franco, M. Santamaria, and F. Di Quarto, *Electron. Lett.* 50, 262 (2014).
29. C. Calì, R. Macaluso, and M. Mosca, *Spectrochim. Acta Part B* 56, 743 (2001).
30. H. Tanaka, T. Shimakawa, T. Miyata, H. Sato, and T. Minami, *Appl. Surf. Sci.* 244, 568 (2005).
31. Joint Committee on Powder Diffraction Standards, Powder Diffraction File No. 036-1451.
32. Y. Kayanuma, *Phys. Rev. B Condens. Matter* 38, 9797 (1988).
33. L. Feng, C. Zhang, G. Gao, and D. Cui, *Nanoscale Res. Lett.* 7, 276 (2012).
34. H. Kim, C.M. Gilmore, A. Pique, J.S. Horwitz, H. Mattoussi, H. Murata, Z.H. Kafai, and D.B. Chrisey, *J. Appl. Phys.* 86, 6451 (1999).
35. H.S. Carranco, G.J. Diaz, M.G. Arellano, J.M. Juárez, G.R. Paredes, and R.P. Sierra, Proceedings of the 5th International Conference on Electrical Engineering, Computing Science and Automatic Control (CCE 2008) IEEE, 421 (2008).
36. Y.-K. Hsu, C.-H. Yu, Y.-C. Chen, and Y.-G. Lin, *J. Power Sources* 242, 541 (2013).
37. Z. Li, Y. Pi, D. Xu, Y. Li, W. Peng, G. Zhang, F. Zhang, and X. Fan, *Appl. Catal. B* 213, 1 (2017).
38. K. Samanta, P. Bhattacharya, and R.S. Katiyar, *J. Appl. Phys.* 108, 113501 (2010).
39. B.S. Mwankemwa, F.J. Nambala, F. Kyeyune, T.T. Hlatshwayo, J.M. Nel, and M. Diale, *Mater. Sci. Semicond. Process.* 71, 209 (2017).
40. J. Gubicza, Practical Applications of X-Ray Line Profile Analysis, in X-Ray Line Profile Analysis in Materials Science (IGI Global, 2014), 292.
41. S. Thamri, I. Sta, M. Jlassi, M. Hajji, and H. Ezzaouia, *Mater. Sci. Semicond. Process.* 71, 310 (2017).
42. V. Postica, I. Hölken, V. Schneider, V. Kaidas, O. Polonskyi, V. Cretu, I. Tiginyanu, F. Faupel, R. Adelung, and O. Lupan, *Mater. Sci. Semicond. Process.* 49, 20 (2016).
43. O. Lupan, S. Shishiyanu, V. Ursaki, H. Khallaf, L. Chow, T. Shishiyanu, V. Sontea, E. Monaico, and S. Railean, *Sol. Energy Mater. Sol. Cells* 93, 1417 (2009).
44. M. Hoppe, N. Ababii, V. Postica, O. Lupan, O. Polonskyi, F. Schütt, S. Kaps, L.F. Sukhodub, V. Sontea, T. Strunskus, F. Faupel, and R. Adelung, *Sens. Actuators B Part* 2, 1362 (2018).
45. E. Muchuweni, T.S. Sathiaraj, and H. Nyakotyo, *J. Alloys Compd.* 721, 45 (2017).
46. S. Hussain, C. Cao, G. Nabi, W.S. Khan, Z. Usman, and T. Mahmood, *Electrochim. Acta* 56, 8342 (2011).
47. J. Tauc, *Optical Properties of Solids* (North Holland: Abeles, 1972).
48. N.H. Ke, P.T.K. Loan, D.A. Tuan, H.T. Dat, C.V. Tran, and L.V.T. Hung, *J. Photochem. Photobiol. A* 349, 100 (2017).
49. S. Inguva, E. Mc Glynn, and J.P. Mosnier, *Thin Solid Films* 621, 171 (2017).

Journal : 11664_JEM | Dispatch : 9-4-2019 | Pages : 8
Article No.: 7195 | ☐ LE ☑ CP | ☐ TYPESET ☑ DISK

50. M. Saad and A. Kassis, *Sol. Energy Mater. Sol. Cells* 79, 507 (2003).
51. W. Siripala, A. Ivanovskaya, T.F. Jaramillo, S.H. Baeck, and E.W. McFarland, *Sol. Energy Mater. Sol. Cells* 77, 229 (2003).
52. H. Kobayashi, H. Mori, T. Ishida, and Y. Nakato, *J. Appl. Phys.* 77, 1301 (1995).
53. A.G. Milnes and D.L. Feucht, *Heterojunctions and Metal-Semiconductor Junctions* (New York: Academic, 1972).
54. W. Niu, M. Zhou, Z. Ye, and L. Zhu, *Sol. Energy Mater. Sol. Cells* 144, 717 (2016).
55. S. Chatterjee, S.K. Saha, and A.J. Pal, *Sol. Energy Mater. Sol. Cells* 147, 17 (2016).

Journal : 11664_JEM | Dispatch : 9-4-2019 | Pages : 8
Article No.: 7195 | ☐ LE ☑ CP | ☐ TYPESET ☑ DISK

Journal : **11664**
Article : **7195**

Author Query Form

Please ensure you fill out your response to the queries raised below and return this form along with your corrections

Author Proof

Dear Author

During the process of typesetting your article, the following queries have arisen. Please check your typeset proof carefully against the queries listed below and mark the necessary changes either directly on the proof/online grid or in the 'Author's response' area provided below

Query	Details Required	Author's Response
AQ1	Kindly check and confirm the affiliation is correctly identified for the author MS Aida and amend if necessary.	
AQ2	Note that 3 to 6 keywords are required for this journal. Kindly adjust the number accordingly.	
AQ3	Please confirm this abbreviation definition added on first use for completeness: JCPDS	